Nat. Hazards Earth Syst. Sci., 9, 1953–1971, 2009
www.nat-hazards-earth-syst-sci.net/9/1953/2009/


Natural Hazards and Earth System Sciences

# Unfolding the procedure of characterizing recorded ultra low frequency, kHZ and MHz electromagetic anomalies prior to the L'Aquila earthquake as pre-seismic ones – Part 1

**K. Eftaxias[1], L. Athanasopoulou[1], G. Balasis[2], M. Kalimeri[1], S. Nikolopoulos[3], Y. Contoyiannis[1], J. Kopanas[1], G. Antonopoulos[1], and C. Nomicos[4]**

[1]Section of Solid State Physics, Department of Physics, Univ. of Athens, Panepistimiopolis, Zografos, 15784, Athens, Greece
[2]Institute for Space Applications and Remote Sensing, National Observatory of Athens, Metaxa and Vas. Pavlou, Penteli, 15236, Athens, Greece
[3]Centre de Recherche de l'ICM, INSERM UMRS 975 – CNRS UMR 7225, Hopital de la Pitie-Salpetriere, Paris, France
[4]Department of Electronics, Technological Educational Institute of Athens, Ag. Spyridonos, Egaleo, 12210, Athens, Greece

Received: 31 July 2009 – Revised: 12 October 2009 – Accepted: 14 October 2009 – Published: 25 November 2009

**Abstract.** Ultra low frequency, kHz and MHz electromagnetic (EM) anomalies were recorded prior to the L'Aquila catastrophic earthquake that occurred on 6 April 2009. The main aims of this paper are threefold: (i) suggest a procedure for the designation of detected EM anomalies as seismogenic ones. We do not expect to be able to provide a succinct and solid definition of a pre-seismic EM emission. Instead, we aim, through a multidisciplinary analysis, to provide the elements of a definition. (ii) Link the detected MHz and kHz EM anomalies with equivalent last stages of the earthquake preparation process. (iii) Put forward physically meaningful arguments for quantifying the time to global failure and the identification of distinguishing features beyond which the evolution towards global failure becomes irreversible. We emphasize that we try to specify not only whether a single EM anomaly is pre-seismic in itself, but also whether a combination of kHz, MHz, and ULF EM anomalies can be characterized as pre-seismic. The entire procedure unfolds in two consecutive parts. Here in Part 1 we focus on the detected kHz EM anomaly, which play a crucial role in our approach to these challenges. We try to discriminate clearly this anomaly from background noise. For this purpose, we analyze the data successively in terms of various concepts of entropy and information theory including, Shannon $n$-block entropy, conditional entropy, entropy of the source, Kolmogorov-Sinai entropy, $T$-entropy, approximate entropy, fractal spectral analysis, R/S analysis and detrended fluctuation analysis. We argue that this analysis reliably distinguishes the candidate kHz EM precursor from the noise: the launch of anomalies from the normal state is combined by a simultaneous appearance of a significantly higher level of organization, and persistency. This finding indicates that the process in which the anomalies are rooted is governed by a positive feedback mechanism. This mechanism induces a non-equilibrium process, i.e., a catastrophic event. This conclusion is supported by the fact that the two crucial signatures included in the kHz EM precursor are also hidden in other quite different, complex catastrophic events as predicted by the theory of complex systems. However, our view is that such an analysis by itself cannot establish a kHz EM anomaly as a precursor. It likely offers necessary but not sufficient criteria in order to recognize an anomaly as pre-seismic. In Part 2 we aim to provide sufficient criteria: the fracture process is characterized by fundamental universally valid scaling relationships which should be reflected in a real fracto-electromagnetic activity. Moreover, we aim to answer the following two key questions: (i) How can we link an individual EM precursor with a distinctive stage of the EQ preparation process; and (ii) How can we identify precursory symptoms in EM observations that indicate that the occurrence of the EQ is unavoidable.

*Correspondence to:* K. Eftaxias
(ceftax@phys.uoa.gr)

Published by Copernicus Publications on behalf of the European Geosciences Union.

## 1 Introduction

A catastrophic earthquake (EQ) occurred on 6 April 2009 (01 h 32 m 41 s UTC) in central Italy (42.33° N–13.33° E). The majority of the damage occurred in the city of L'Aquila.

A vital problem in material science and in geophysics is the identification of precursors of macroscopic defects or shocks. An EQ is essentially a large scale fracture so, as with any physical phenomenon, science should have some predictive power regarding its future behaviour.

Earthquake physicists attempt to link the available observations to the processes occurring in the Earth's crust. Fracture-induced physical fields allow a real-time monitoring of damage evolution in materials during mechanical loading. When a material is strained, electromagnetic (EM) emissions in a wide frequency spectrum ranging from kHz to MHz are produced by opening cracks, which can be considered as so-called precursors of general fracture. These precursors are detectable both on a laboratory and a geological scale (Bahat et al., 2005; Eftaxias et al., 2007a; Hayakawa and Fujinawa,1994; Hayakawa, 1999; Hayakawa and Molchanov, 2002).

Since 1994, a station has been installed and operating at a mountainous site of Zante Island in the Ionian Sea (Western Greece). Its purpose is the detection of EM precursors. Clear ultra-low-frequency (ULF), kHz and MHz precursors have been detected over periods ranging from a few days to a few hours prior to catastrophic EQs that have occurred in Greece since its installation.

*We emphasize that the detected precursors were associated with EQs that occurred in land (or near the coast-line), and were strong (magnitude 6 or larger) and shallow* (Contoyiannis et al., 2005; Karamanos et al., 2006). Recent results indicate that the recorded EM precursors contain information characteristic of an ensuing seismic event (e.g., Eftaxias et al., 2002, 2004, 2006, 2007; Kapiris et al., 2004, 2005; Contoyiannis et al., 2005; Contoyiannis and Eftaxias, 2008; Kalimeri et al., 2008; Papadimitriou et al., 2008).

The L'Aquila EQ occurred in land, was very shallow and its magnitude was 6.3. MHz, kHz and ULF EM anomalies were observed before this EQ. An important feature, observed both on a laboratory and a geological scale, is that the MHz radiation precedes the kHz one (Eftaxias et al., 2002 and references therein). The detected anomalies followed the temporal scheme listed below.

(i) The MHz EM anomalies were detected on 26 March 2009 and 2 April 2009.

(ii) The kHz EM anomalies emerged on 4 April 2009.

(iii) The ULF EM anomaly was continuously recorded from 29 March 2009 up to 2 April 2009.

We point out that despite fairly abundant circumstantial evidence, pre-seismic EM signals have not been adequately accepted as real physical quantities. Many of the problems of fundamental importance in seismo-EM signals are unsolved. Thus, the question naturally arises as to whether the recorded anomalies were seismogenic or not.

We stress that the experimental arrangement affords us the possibility of determining not only whether or not a single kHz, MHz, or ULF EM anomaly is pre-seismic in itself, but also whether a combination of such kHz, MHz, and ULF anomalies can be characterized as pre-seismic. Some key open questions are the following.

(i) How can we recognize an EM observation as a pre-seismic one? We wonder whether necessary and sufficient criteria have been established that permit the characterization of an EM observation as a precursor.

(ii) How can we link an individual EM precursor with a distinctive stage of the EQ preparation process?

(iii) How can we identify precursory symptoms in EM observations that indicate that the occurrence of the EQ is unavoidable?

Here we shall study the possible seismogenic origin of the anomalies recorded prior to the L'Aquila EQ within the frame work of these *key questions*.

Recent studies have provided us with relevant experience (e.g., Kapiris et al., 2004; Contoyiannis et al., 2005, 2008; Papadimitriou et al., 2008; Eftaxias et al., 2006, 2007, 2009a). This experience affords us the possibility of verifying the results of the present study by comparing it with the results of previous ones.

Here, in Part 1, we present our procedure for answering key question (i) above. This procedure applies to both the kHz and MHz anomalies, but for now we restrict our study to the kHz anomaly. In Part II we focus on the MHz and ULF EM anomalies and key questions (ii) and (iii).

*Our approach*. An anomaly in a recorded time series is defined as a deviation from normal (background) behaviour. In order to develop a quantitative identification of EM precursors, concepts of entropy and tools of information theory are used in order to identify statistical patterns. It is expected that a significant change in the statistical pattern represents a deviation from normal behaviour, revealing the presence of an anomaly. Symbolic dynamics provides a rigorous way of looking at "real" dynamics. First, we attempt a symbolic analysis of experimental data in terms of Shannon $n$-block entropy, Shannon $n$-block entropy per letter, conditional entropy, entropy of the source, and $T$-entropy. It is well-known that Shannon entropy works best in dealing with systems composed of subsystems which can access all the available phase space and which are either independent or interact via short-range forces. For systems exhibiting long-range correlations, memory, or fractal properties, Tsallis' entropy becomes the most appropriate mathematical tool (Tsallis, 1988, 2009). A central property of the EQ preparation process is the possible occurrence of coherent large-scale collective behaviour with a very rich structure, resulting from repeated

nonlinear interactions among the constituents of the system (Sornette, 1999). Consequently, Tsallis entropy is an appropriate tool for investigating the launch of an EM precursor.

The results show that all the techniques based on symbolic dynamics clearly discriminate the recorded kHz anomalies from the background: they are characterized by a significantly lower complexity (or higher organization).

For purpose of comparison we also analyze the data by means of Approximate Entropy ($ApEn$), which refers just to the raw data. This analysis verifies the results of symbolic dynamics.

Fractal spectral analysis offers additional information concerning signal/noise discrimination by doing two things. (i) It shows that the candidate kHz precursor follows the fractional Brownian motion (fBm)-model while, on the contrary, the background follows the 1/f-noise model. (ii) It implies that the candidate kHz precursor has *persistent* behaviour. The existence of persistency in the candidate precursor is confirmed by R/S analysis, while the conclusion that the anomaly follows the persistent fBm-model is verified by Detrended Fluctuation Analysis.

The abrupt simultaneous appearance of both high organization and persistency in a launched kHz anomaly implies that the underlying fracto-electromagnetic process is governed by a positive feedback mechanism (Sammis and Sornette, 2002). Such a mechanism is consistent with the anomaly's being a candidate precursor.

The paper is organized as follows. Section 2 briefly describes the configuration of the Zante station. It also presents the candidate ULF, kHz and MHz EM precursors. Section 3 refers to theoretical background of the present study. More precisely, it introduces the idea of symbolic dynamics and provides a brief overview of (Shannon-like) $n$-block entropy, differential or conditional entropy, entropy of the source or limit entropy, and Kolmogorov-Sinai entropy, nonextensive Tsallis entropy, $T$-entropy, approximate entropy, fractal spectral analysis, R/S analysis, and fractal detrended analysis. In Sect. 4 all the aforementioned methods of analysis are applied to the data. Section 5 discusses the results in terms of the theory of complex systems. Finally, Sect. 6 summarizes and concludes the paper.

## 2 Data presentation

Since 1994, a station has been functioning at a mountainous site of Zante island (37.76° N–20.76° E) in the Ionian Sea (western Greece) with the following configuration: (i) six loop antennas detecting the three components (EW, NS, and vertical) of the variations of the magnetic field at 3 kHz and 10 kHz respectively; (ii) two vertical $\lambda/2$ electric dipole antennas detecting the electric field variations at 41 and 54 MHz respectively, and (iii) two Short Thin Wire Antennas (STWA) of 100 m length each, lying on the Earth's surface, detecting ultra low frequency (ULF) (<1 Hz) anomalies in the EW and NS directions respectively. The 3 kHz, 10 kHz, 41 MHz, and 54 MHz were selected in order to minimize the effects of the man-made noise in the mountainous area of Zante. All the EM time-series were sampled once per second, i.e sampling frequency 1 Hz. The distance between the Zante station and the epicentre of the L'Aquila EQ is approximately 800 km.

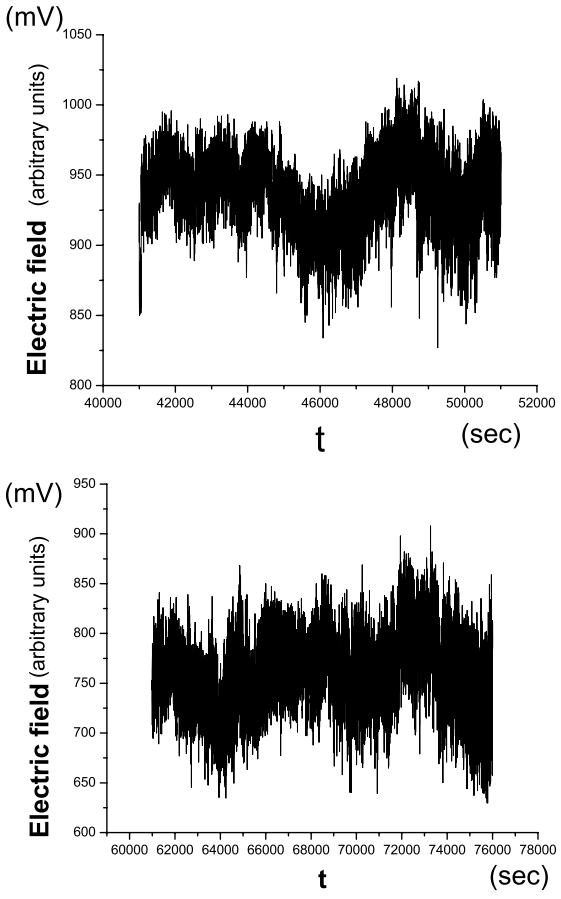


**Fig. 1.** Critical excerpts of the 41 MHz electric field strength time series on 26 March 2009 (upper panel) and 2 April 2009 (lower panel), respectively. The behaviour of the EM fluctuations included in each time interval is analogous to a continuous (second order) phase transition. The vertical axis shows the output of sensor (in mV) that measures the electric field.

A sequence of MHz, kHz and ULF EM anomalies were observed one after the other before the L'Aquila EQ, as follows.

### 2.1 MHz EM anomalies

EM anomalies were simultaneously recorded at 41 MHz and 54 MHz on 26 March 2009 and 2 April 2009. Figure 1 shows excerpts of the recorded anomalies by the 41 MHz electric dipole. In Part 2 we will show that the excerpts of the recorded MHz EM emission presented in Fig. 1 may be described in analogy with a thermal continuous (second order) phase transition (Eftaxias et al., 2009b).

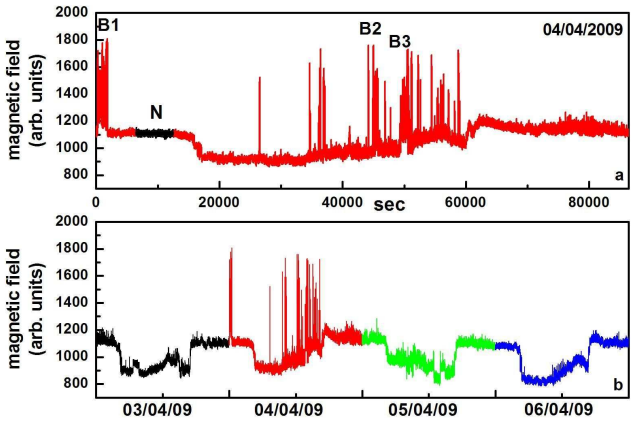


**Fig. 2.** **(a)** We observed the presence of a sequence of strong EM impulsive bursts at 10 kHz on 4 April 2009. **(b)** These anomalies were launched during a quiescent period in the detection of EM disturbances in the kHz band. A segment from the EM background (N) and three excerpts of the emerged strong kHz EM activity (B1, B2, B3) from this time series are indicated. The vertical axis shows the output of sensor (in mV) that measures the magnetic field.

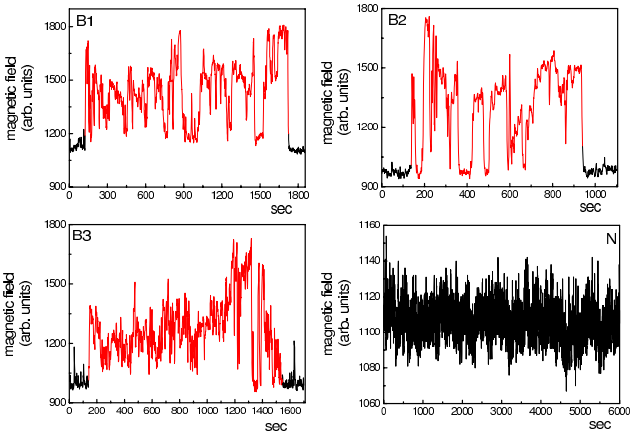


**Fig. 3.** Magnified images of the excerpts N, B1, B2, and B3 that are shown in Fig. 2.

### 2.2 kHz EM anomalies

A sequence of strong multi-peaked EM bursts, with sharp onsets and ends, were simultaneously recorded by the 3 kHz and 10 kHz loop antennas on 4 April 2009. Figure 2a shows the EM anomalies recorded by the 10 kHz (E-W) loop antenna. These anomalies were launched over a quiescent period concerning the detection of EM disturbances at the kHz frequency band (Fig. 2b). Figure 3 depicts magnified images of the excerpts N, B1, B2, and B3 that are shown in Fig. 2a.

### 2.3 ULF EM anomaly

The daily pattern of the ULF recordings during the normal period, i.e., far from the EQ occurrence, follows a rather periodical variation which is characterized by the existence of a clear minimum during the day time (Fig. 4). One finds a clear alteration of the normal daily profile as the shock approaches. The ULF EM anomaly continuously appeared from 29 March 2009 up to 2 April 2009. The curve returns to its normal shape on 7 April 2009. In Part 2 we will show that this anomaly may be originated in seismo-ionospheric anomalous states which produce changes on EM wave propagation. Importantly, based on very low frequency (kHz) radio sounding, Biagi et al. (2009) and Rozhnoi et al. (2009) have observed ionospheric perturbations in the time interval 2–8 days before the L'Aquila EQ.

We note that all of the recorded EM anomalies we report here have been obtained during a quiet period in terms of magnetic storm, solar flares and atmospheric activity. In addition, the consecutive appearance of ULF, MHz and kHz EM anomalies in a time interval of a few days prior to the L'Aquila EQ occurrence excludes the possibility that they were man-made.

## 3 Theoretical background

In this section we briefly introduce concepts of entropy and tools of information theory which will be used in the present study.

### 3.1 Fundamentals of symbolic dynamics

For the scale of completeness and for later use, we compile here the basic points of symbolic dynamics. Symbolic time series analysis is a useful tool for modelling and characterization of nonlinear dynamical systems (Voss et al., 1996). It provides a rigorous way of looking at "real" dynamics with finite precision (Hao, 1989, 1991; Kitchens, 1998; Karamanos and Nicolis, 1999). Briefly, it is a way of coarse-graining or simplifying the description.

The basic idea is quite simple. One divides the phase space into a finite number of partitions and labels each partition with a symbol (e.g. a letter from some alphabet). Instead of representing the trajectories by infinite sequences of numbers-iterates from a discrete map or sampled points along the trajectories of a continuous flow, one watches the alteration of symbols. Of course, in so doing one loses an amount of detailed information, but some of the invariant, robust properties of the dynamics may be kept, e.g. periodicity, symmetry, or the chaotic nature of an orbit (Hao, 1991).

In the framework of symbolic dynamics, time series are transformed into a series of symbols by using an appropriate partition which results in relatively few symbols. After symbolization, the next step is the construction of "symbol sequences" ("words" in the language symbolic dynamics) from the symbol series by collecting groups of symbols together in temporal order.

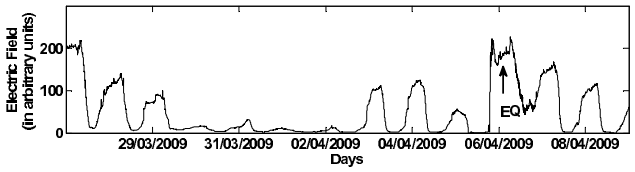


**Fig. 4.** The time series of the ULF electric field strength, as recorded by the STWA sensors. The vertical axis shows the output of sensor (in mV) that measures the electric field.

To be more precise, the simplest possible coarse-graining of a time series is given by choosing a threshold $C$ (usually the mean value of the data considered) and assigning the symbols "1" and "0" to the signal, depending on whether it is above or below the threshold (binary partition). Thus, we generate a symbolic time series from a 2-letter ($\lambda$=2) alphabet (0, 1), e.g. 0110100110010110…. We usually read this symbolic sequence in terms of distinct consecutive "blocks" (words) of length $n=2$. In this case one obtains 01/10/10/01/10/01/01/10/…. We call this reading procedure "lumping".

The number of all possible kinds of words is $\lambda^n=2^2=4$, namely 00, 01, 10, 11. The required probabilities for the estimation of an entropy, $p_{00}$, $p_{01}$, $p_{10}$, $p_{11}$ are the fractions of the blocks (words) 00, 01, 10, 11 in the symbolic time series, namely, 0, 4/16, 4/16, and 0, correspondingly. Based on these probabilities we can estimate, for example, the probabilistic entropy measure $H_S$ introduced by Shannon (1948),

$$H_S = -\sum p_i \ln p_i \tag{1}$$

where $p_i$ are the probabilities associated with the microscopic configurations.

Various tools of information theory and entropy concepts are used to identify statistical patterns in the symbolic sequences, onto which the dynamics of the original system under analysis has been projected. *For detection of an anomaly, it suffices that a detectable change in the pattern represents a deviation of the system from nominal behaviour (Graben and Kurths, 2003).* Recent published work has reported novel methods for detection of anomalies in complex dynamical systems, which rely on symbolic time series analysis. Entropies depending on the word-frequency distribution in symbolic sequences are of special interest, extending Shannon's classical definition of the entropy and providing a link between dynamical systems and information theory. These entropies take a large/small value if there are many/few kinds of patterns, i.e. they decrease while the organization of patterns is increasing. In this way, these entropies can measure the complexity of a signal.

*It is important to note that one cannot find an optimum organization or complexity measure (Kurths et al., 1995). We think that a combination of some such quantities which refer to different aspects, such as structural or dynamical properties, is the most promising way. In this way several well-known techniques have been applied to extract EM precursors hidden in kHz EM time series.*

### 3.2 The concept of dynamical (Shannon-like) $n$-block entropies

Block entropies, depending on the word-frequency distribution, are of special interest, extending Shannon's classical definition of the entropy of a single state to the entropy of a succession of states (Nicolis and Gaspard, 1994).

Symbolic sequences, $\{A_1 \ldots A_n \ldots A_L\}$, are composed of letters from an alphabet consisting of $\lambda$ letters $\{A^{(1)}, A^{(2)} \ldots A^{(\lambda)}\}$. An English text for example, is written on an alphabet consisting of 26 letters $\{A, B, C \ldots X, Y, Z\}$.

A word of length $n<L$, $\{A_1 \ldots A_n\}$, is defined by a substring of length $n$ taken from $\{A_1 \ldots A_n \ldots A_L\}$. The total number of different words of length $n$ which exists in the alphabet is

$$N_{\lambda n} = \lambda^n.$$

We specify that the symbolic sequence is to be read in terms of distinct consecutive "blocks" (words) of length $n$,

$$\ldots \underbrace{A_1 \ldots A_n}_{B_1} \underbrace{A_{n+1} \ldots A_{2n}}_{B_2} \ldots \underbrace{A_{jn+1} \ldots A_{(j+1)n}}_{B_{j+1}} \ldots \tag{2}$$

As stated previously, we call this reading procedure *lumping*. *Gliding* is the reading of the symbolic sequence using a *moving frame*. It has been suggested that, at least in some cases, the entropy analysis by lumping is much more sensitive than classical entropy analysis (gliding) (Karamanos, 2000, 2001).

The probability $p^{(n)}(A_1, \ldots, A_n)$ of occurrence of a block $A_1 \ldots A_n$ is defined by the fraction,

$$\frac{\text{No. of blocks, } A_1 \ldots A_n, \text{ encountered when lumping}}{\text{total No. of blocks}} \tag{3}$$

starting from the beginning of the sequence.

The following quantities characterize the information content of the symbolic sequence (Khinchin, 1957; Ebeling and Nicolis, 1992).

#### 3.2.1 The Shannon $n$-block entropy

Following Shannon's approach (Shannon, 1948) the $n$-block entropy, $H(n)$, is given by

$$H(n) = -\sum_{(A_1, \ldots, A_n)} p^{(n)}(A_1, \ldots, A_n) \cdot \ln p^{(n)}(A_1, \ldots, A_n). \tag{4}$$

*The entropy H(n) is a measure of uncertainty and gives the average amount of information necessary to predict a subsequence of length n.*

#### 3.2.2 The Shannon $n$-block entropy per letter

From the Shannon $n$-block entropy we derive the $n$-block entropy per letter

$$h^{(n)} = \frac{H(n)}{n}. \quad (5)$$

*This entropy may be interpreted as the average uncertainty per letter of an n-block.*

#### 3.2.3 The conditional entropy

From the Shannon $n$-block entropies we derive the conditional (dynamic) entropies by the definition

$$h_{(n)} = H(n+1) - H(n). \quad (6)$$

*The conditional entropy $h_{(n)}$ measures the uncertainty of predicting a state one step into the future, provided a history of the preceding n states.*

Predictability is measured by conditional entropies. For Bernoulli sequences we have the maximal uncertainty

$$h_{(n)} = \log(\lambda). \quad (7)$$

Therefore we define the difference

$$r_n = log(\lambda) - h_{(n)} \quad (8)$$

as the average predictability of the state following a measured $n$-trajectory. *In other words, predictability is the information we get by exploration of the next state in comparison to the available knowledge.*

We use, in most cases, $\lambda$ as the base of the logarithms. Using this base the maximal uncertainty/predictability is one (Ebeling, 1997).

In general our expectation is that any long-range memory decreases the conditional entropies and improves our chances for prediction.

(iv) *The entropy of the source or limit entropy*

A quantity of particular interest is the entropy of the source, defined as

$$h = \lim_{n\to\infty} h_{(n)} = \lim_{n\to\infty} h^{(n)} \quad (9)$$

*It is the average amount of information necessary to predict the next symbol when being informed about the complete pre-history of the system*.

The limit entropy $h$ is the discrete analog of Kolmogorov-Sinai entropy. Since positive Kolmogorov-Sinai entropy implies the existence of a positive Lyapunov exponent, it is an important measure of chaos.

### 3.3 Principles of non-extensive Tsallis entropy

In the Introduction we explained why physical systems that are characterized by long-range interactions or long-term memories, or are of a multi-fractal nature, are best described by a generalized statistical-mechanical formalism proposed by Tsallis (1988, 2009). More precisely, inspired by multifractals concepts, he introduced an entropic expression characterized by an index $q$ which leads to non-extensive statistics (1988, 2009):

$$S_q = k\frac{1}{q-1}\left(1 - \sum_{i=1}^{W} p_i^q\right), \quad (10)$$

where $p_i$ are probabilities associated with the microscopic configurations, $W$ is their total number, $q$ is a real number and $k$ is Boltzmann's constant.

The entropic index $q$ describes the deviation of Tsallis entropy from the standard Boltzmann-Gibbs one. Indeed, using $p_i^{(q-1)} = e^{(q-1)\ln(p_i)} \sim 1+(q-1)\ln(p_i)$ in the limit $q\to 1$, we recover the usual Boltzmann-Gibbs entropy

$$S_1 = -k\sum_{i=1}^{W} p_i \ln(p_i). \quad (11)$$

The entropic index $q$ characterizes the degree of non-extensivity reflected in the following pseudo-additivity rule:

$$S_q(A+B) = S_q(A) + S_q(B) + \frac{1-q}{k} S_q(A) S_q(B). \quad (12)$$

For subsystems that have special probability correlations, extensivity

$$S_{B-G} = S_{B-G}(A) + S_{B-G}(B) \quad (13)$$

is not valid for $S_{B-G}$, but may occur for $S_q$ with a particular value of the index $q$. Such systems are sometimes referred to as non-extensive (Tsallis, 1988, 2009).

The cases $q>1$ and $q<1$, correspond to sub-additivity, or super-additivity, respectively. We may think of $q$ as a bias-parameter: $q<1$ privileges rare events, while $q>1$ privileges prominent events (Zunino et al., 2008).

We clarify that the parameter $q$ itself is not a measure of the complexity of the system but measures the degree of non-extensivity of the system. It is the time variations of the Tsallis entropy for a given $q$, ($S_q$), that quantify the dynamic changes of the complexity of the system. *Lower $S_q$ values characterize the portions of the signal with lower complexity*.

In terms of symbolic dynamics the Tsallis entropy for the word length $n$ is (Kalimeri et al., 2008):

$$S_q(n) = k\frac{1}{q-1}\left(1 - \sum_{(A_1,A_2,\ldots,A_n)} [p(n)_{A_1,A_2,\ldots,A_n}]^q\right). \quad (14)$$

### 3.4 $T$-entropy of a string

$T$-entropy is a novel grammar-based complexity/information measure defined for finite strings of symbols (Ebeling et al., 2001; Tichener et al., 2005). It is a weighted count of the number of production steps required to construct a string

from its alphabet. *Briefly, it is based on the intellectual economy one makes when rewriting a string according to some rules*.

An example of an actual calculation of the $T$-complexity for a finite string is given by Ebeling et al. (2001). We briefly describe how the $T$-complexity is computed for finite strings. The $T$-complexity of a string is defined by the use of one recursive hierarchical pattern copying (RHPC) algorithm. It computes the effective number of $T$-augmentation steps required to generate the string. The $T$-complexity may thus be computed effectively from any string and the resultant value is unique.

The string $x(n)$ is parsed to derive constituent patterns $p_i \in A^+$ and associated copy-exponents $k_i \in N^+, i=1,2,\ldots,q$, where $q \in N^+$ satisfying:

$$x = p_q^{k_q} p_{q-1}^{k_{q-1}} \ldots p_i^{k_i} \ldots p_1^{k_1} \alpha_0, \quad \alpha_0 \in A. \tag{15}$$

Each pattern $p_i$ is further constrained to satisfy:

$$p_i = p_{i-1}^{m_{i,i-1}} p_{i-2}^{m_{i,i-2}} \ldots p_j^{m_{i,j}} \ldots p_1^{m_{i,1}} \alpha_i, \tag{16}$$

$$\alpha_i \in A \quad \text{and} = 0 \leq m_{i,j} \leq k_j. \tag{17}$$

The $T$-complexity $C_T(x(n))$ is defined in terms of the copy-exponents $k_i$:

$$C_T(x(n)) = \sum_i^q \ln(k_i + 1). \tag{18}$$

One may verify that $C_T(x(n))$ is minimal for a string comprising a single repeating character.

The $T$-information $I_T(x(n))$ of the string $x(n)$ is defined as the inverse logarithmic integral, $li^{-1}$, of the $T$-complexity divided by a scaling constant ln2:

$$I_T(x(n)) = li^{-1}\left(\frac{C_T(x(n))}{\ln 2}\right). \tag{19}$$

In the limit $n \to \infty$ we have that $I_T(x(n)) \leq \ln(\#A^n)$.

The form of the right-hand side may be recognizable as the maximum possible $n$-block entropy of Shannon's definition. The Naperian logarithm implicitly gives to the $T$-information the units of nats. $I_T(x(n))$ is the $T$-information of string $x(n)$. The *average $T$-information rate per symbol*, referred to here as the average $T$-entropy of $x(n)$ and denoted by $h_T(x(n))$, is defined along similar lines,

$$h_T(x(n)) = \frac{I_T(x(n))}{n} (\text{nats/symbol}). \tag{20}$$

### 3.5 Approximate entropy

Related to time series analysis, the approximate entropy, $ApEn$, provides a measure of the degree of irregularity or randomness within a series of data (of length $N$). $ApEn$ was pioneered by Pincus as a measure of system complexity (Pincus, 1991). It was introduced as a quantification of regularity in relatively short and noisy data. It is rooted in the work of Grassberger and Procaccia (1983) and has been widely applied to biological systems (Pincus and Goldberger, 1994; Pincus and Singer, 1996, and references therein).

The approximate entropy examines time series for similar epochs: more similar and more frequent epochs lead to lower values of $ApEn$.

For a qualitative point of view, given $N$ points, the $ApEn$-like statistics is approximately equal to the negative logarithm of the conditional probability that two sequences that are similar for $m$ points remain similar, that is, within a tolerance $r$, at the next point. Smaller $ApEn$-values indicate a greater chance that a set of data will be followed by similar data (regularity), thus, smaller values indicate greater regularity. Conversely, a greater value for $ApEn$ signifies a lesser chance of similar data being repeated (irregularity), hence, greater values convey more disorder, randomness and system complexity. Thus a low/high value of $ApEn$ reflects a high/low degree of regularity. Notably, $ApEn$ detects changes in underlying episodic behaviour not reflected in peak occurrences or amplitudes (Pincus and Keefe, 1992).

The following is a short description of the calculation of $ApEn$. A more comprehensive description of $ApEn$ may be found in (Pincus, 1991; Pincus and Goldberger, 1994; Pincus and Singer, 1996).

Given any sequence of data points $u(i)$ from $i=1$ to $N$, it is possible to define vector sequences $x(i)$, which consists of length $m$ and are made up of consecutive $u(i)$, specifically defined by the following:

$$x(i) = (u[i], u[i+1], \ldots, u[i+m-1]). \tag{21}$$

In order to estimate the frequency that vectors $x(i)$ repeat themselves throughout the data set within a tolerance $r$, the distance $d(x[i], x[j])$ is defined as the maximum difference between the scalar components $x(i)$ and $x(j)$. Explicitly, two vectors $x(i)$ and $x(j)$ are "similar" within the tolerance or filter $r$, namely $d(x[i], x[j]) \leq r$, if the difference between any two values for $u(i)$ and $u(j)$ within runs of length $m$ does not exceed $r$ (i.e. $|u(i+k) - u(j+k)| \leq r$ for $0 \leq k \leq m$). Subsequently, the correlation sum of vector $x(i)$ is

$$C_i^m(r) = \frac{[\text{number of } \ j \ \text{ such that } \ d(x[i], x[j]) \leq r]}{(N-m+1)},$$

where $j \leq (N-m+1)$.

The $C_i^m(r)$ values measure, within a tolerance $r$, the regularity (frequency) of patterns similar to a given one of window length $m$. The parameter $r$ acts like a filter value: within resolution $r$, the numerator count the number of vectors that are approximately the same as a given vector $x(i)$. The quantity $C_i^m(r)$ is called the correlation sum because it quantifies the summed (or global) correlation of vector $x(i)$ with all other vectors.

Taking the natural logarithm of $C_i^m(r)$, the mean logarithmic correlation sum of all vectors is defined as:

$$\Phi^m(r) = \sum_i lnC_i^m(r)/(N-m+1) \quad (22)$$

where $\sum_i$ is a sum from $i=1$ to $(N-m+1)$. $\Phi^m(r)$ is a measure of the prevalence of repetitive patterns of length $m$ within the filter $r$. Briefly, $\Phi^m(r)$ represents the average frequency of all the $m$-point patterns in the sequence remain close to each other.

Finally, approximate entropy, or $ApEn(m,r,N)$, is defined as the natural logarithm of the relative prevalence of repetitive patterns of length $m$ as compared with those of length $m+1$:

$$ApEn(m,r,N) = \Phi^m(r) - \Phi^{m+1}(r). \quad (23)$$

Thus, $ApEn(m,r,N)$ measures the logarithmic frequency that similar runs (within the filter $r$) of length $m$ also remain similar when the length of the run is increased by 1. Small values of $ApEn$ indicate regularity, given that increasing run length $m$ by 1 does not decrease the value of $\Phi^m(r)$ significantly (i.e., regularity connotes that $\Phi^m[r] \approx \Phi^{m+1}[r]$). $ApEn(m,r,N)$ is expressed as a difference, but in essence it represents a ratio; note that $\Phi^m[r]$ is a logarithm of the averaged $C_i^m(r)$, and the ratio of logarithms is equivalent to their difference.

*In summary, ApEn is a "regularity statistics" that quantifies the unpredictability of fluctuations in a time series. The presence of repetitive patterns of fluctuation in a time series renders it more predictable than a time series in which such patterns are absent. A time series containing many repetitive patterns has a relatively small ApEn; a less predictable (i.e., more complex) process has a higher ApEn.*

### 3.6 Fractal spectral analysis

It is well known that during the complex process of EQ preparation, linkages between space and time produce characteristic fractal structures. It is expected that these fractal structures are included in signals rooted in the EQ generation process.

If a time series is a temporal fractal then a power-law of the form $S(f) \propto f^{-\beta}$ is obeyed, with $S(f)$ the power spectral density and $f$ the frequency. The spectral scaling exponent $\beta$ is a measure of the strength of time correlations. The goodness of the power law fit to a time series is represented by a linear correlation coefficient, $r$.

Our attention is directed to whether distinct changes in the scaling exponent $\beta$ emerge in kHz EM bursts. For this purpose, we applied the wavelet analysis technique to derive the coefficients of its power spectrum. The wavelet transform provides a representation of the signal in both the time and frequency domains. In contrast to the Fourier transform, which provides a description of the overall regularity of signals, the wavelet transform identifies the temporal evolution of various frequencies in a time-frequency plane that indicates the frequency content of a signal a given time. The decomposition pattern of the time-frequency plane is determined by the choice of basis functions. In the present study, we used the continuous wavelet transform with the Morlet wavelet as basis function. The results were checked for consistency using the Paul and DOG mother functions (Torrence and Compo, 1998).

### 3.7 Rescaled Range Analysis: the Hurst exponent

The Rescaled Range Analysis (R/S), which was introduced by Hurst (1951), attempts to find patterns that might repeat in the future. There are two main variables used in this method, the range of the data (as measured by the highest and lowest values in the time period) and the standard deviation of the data.

Hurst, in his analysis, first transformed the natural records in time $X(N) = x(1), x(2), \ldots, x(N)$, into a new variable $y(n,N)$, the so-called accumulated departure of the natural record in time in a given year $n (n = 1, 2, \ldots N)$, from the average, $< x(n)$, over a period of $N$ years. The transformation follows the formula

$$y(n,N) = \sum_{i=1}^{n} (x(i) - \langle x \rangle) \quad (24)$$

Then, he introduced the rescaled range

$$R/S = \frac{R(N)}{S(N)} \quad (25)$$

in which the range $R(N)$ is defined as a distance between the minimum and maximum value of $y$ by

$$R(N) = y_{\max} - y_{\min} \quad (26)$$

and the standard deviation $S(N)$ by

$$S(N) = \sqrt{\frac{1}{N}\sum_{i=1}^{N}[y(i) - \langle x \rangle]^2} \quad (27)$$

R/S is expected to show a power-law dependence on the bin size $n$:

$$R(n)/S(n) \sim n^H, \quad (28)$$

where $H$ is the Hurst exponent.

### 3.8 Detrended Fluctuation Analysis

Often experimental data are affected by non-stationary behavior, and strong trends in the data can lead to a false detection of long-range correlations if the results are not carefully interpreted. Detrended Fluctuation Analysis (DFA), proposed by Peng et al. (1993, 1994, and 1995) and based on random walk theory, is a well-established method for determining the scaling behaviour of noisy data in the presence of trends without knowing their origin and shape.

We briefly introduce the DFA method, which involves the following six steps.

(i) We consider a time series $i = 1, \ldots, N$ of length $N$. In most applications, the index $i$ will correspond to the time of measurements. We are interested in the correlation of the values $x_i$ and $x_{i+k}$ for different time lags, i.e. correlations over different time scales $k$. In the first step, we determine the integrated profile

$$y(k) = \sum_{i=1}^{k} (x(i) - \langle x \rangle), i = 1, \ldots, N \quad (29)$$

where $\langle \ldots \rangle$ denotes the mean.

(ii) The integrated signal $y(k)$ is divided into non-overlapping bins of equal length $n$.

(iii) In each bin of length $n$, we fit $y(k)$, using a polynomial function of order $l$, which represents the trend in that box. We usually use a linear fit. The $y$ coordinate of the fit line in each box is denoted by $y_n(k)$.

(iv) The integrated signal $y(k)$ is detrended by subtracting the local trend $y_n(k)$. Then we define the detrended time series for bins of duration $n$, by $y_n(k) = y(k) - y_n(k)$.

(v) For a given bin size $n$, the root-mean-square (rms) fluctuations for this integrated and detrended signal is calculated:

$$F(n) = \sqrt{\frac{1}{N} \sum_{k=1}^{N} \{y(k) - n(k)\}^2} \quad (30)$$

(vi) The aforementioned computation is repeated for a broad range of scales box sizes ($n$) to provide a relationship between $F(n)$ and the box size $n$.

A power-law relation between the average root-mean square fluctuation $F(n)$ and the bin size $n$ indicates the presence of scaling:

$$F(n) \sim n^{\alpha} \quad (31)$$

The scaling exponent $\alpha$ quantifies the strength of the long-range power-law correlations in the time series.

## 4 Application to the data

In this section, we apply all the methods described in section 3 to the kHz EM time series under study.

### 4.1 Dynamical characteristics of pre-seismic kHz EM activity in terms of block entropies

The upper panel in Fig. 5 shows the entropies obtained by *lumping*. The lower panel depicts the entropies estimated by *gliding*. We mentioned that *lumping* is the reading of the symbolic sequence by taking *portions*, as opposed to *gliding* where one has essentially a *moving frame*. We conclude that both methods of reading lead to consistent results.

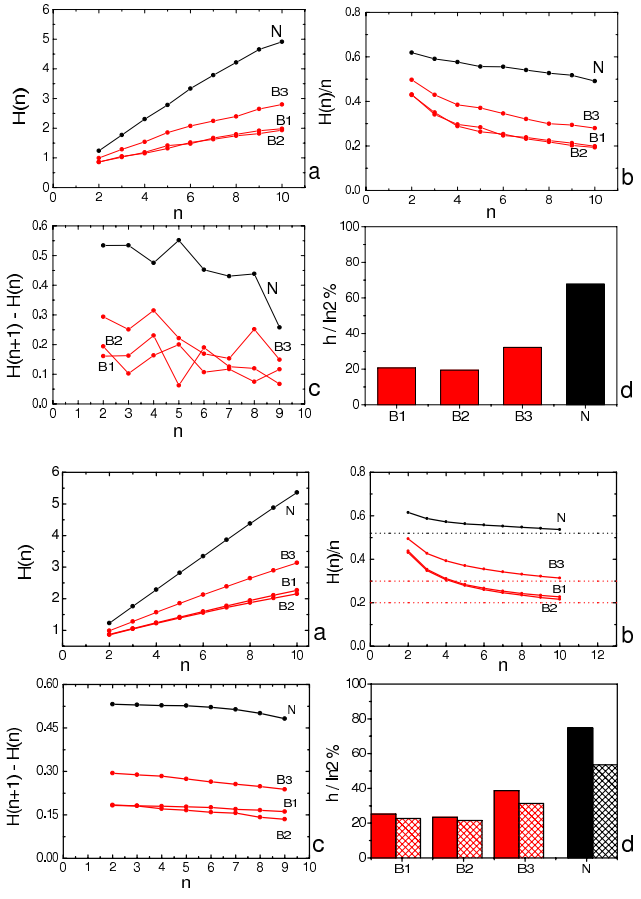


**Fig. 5.** The Shannon $n$-block entropy $H(n)$ **(a)**, Shannon $n$-block entropy per letter $H(n)/n$ **(b)**, conditional entropy $H(n+1)-H(n)$ **(c)**, and Kolmogorov entropy $h/ln2$ **(d)** in the background noise (N) and the three candidate precursory EM bursts B1, B2, B3 for lumping (upper panel) and gliding (lower panel). All these symbolic entropies, for either reading technique, show a significant drop of complexity in the EM bursts compared to the noise.

#### 4.1.1 The Shannon $n$-block entropy

Figure 5a depict the Shannon $n$-block entropy, $H(n)$, as a function of the word length $n$ for the time windows N, B1, B2, and B3 (see Fig. 3). We observe that the noise N is characterized by significantly larger $H(n)$-values.

*This finding means that the average amount of information necessary to predict a sub-sequence of length n is larger in the noise than in the bursts B1, B2, and B3 is.*

#### 4.1.2 The Shannon $n$-block entropy per letter

Figure 5b show that *the average uncertainty per letter of an n-block is larger in the noise than in the bursts B1, B2, and B3 is.*

#### 4.1.3 The conditional entropy

Figsure 5c illustrate the conditional entropies, $h_{(n)}$, as a function of the word length $n$ for the excerpts under study. The noise N has significantly higher $h_{(n)}$-values.

*This result means that the uncertainty of predicting one step in the future, provided a history of the present state and the previous n-1 states, is higher in the case of noise N or, in terms of predictability, the average predictability of the state following after a measured n-trajectory is higher in the bursts B1, B2, and B3. We recall that any long-range memory decreases the conditional entropies and improves the chances for predictions.*

#### 4.1.4 The entropy of the source

One important conjecture, due essentially to Ebeling and Nicolis (1992), is that the most general (asymptotic) scaling of the block entropies takes the form

$$H(n) = e + nh + gn^{\mu_0}(lnn)^{\mu_1} \tag{32}$$

where $e$ and $g$ are constants and $\mu_0$ and $\mu_1$ are constant exponents.

Because of the rather linear scaling observed in Fig. 5a, we approximate the former equation by the simple linear relation

$$H(n) = e + nh \tag{33}$$

With this approximation, the slops of the lines in Fig. 5a can be considered as the entropy of the source, which is the discrete analog of the Kolmogorov-Sinai entropy. Since the source entropy lies between zero and ln2 we can express it as a percentage by multiplying by (100/ln2).

Figure 5a (upper panel) shows that there is a clear distinction of the values of the slopes, leading to a significant difference in the corresponding Kolmogorov-Sinai entropies (Fig. 5d, upper panel).

Now lets focus on the entropies estimated by gliding (Fig. 5, lower panel). In this lower panel we show the Kolmogorov-Sinai entropy (Fig. 5d, solid columns) estimated by:

(i) The slope of $H(n)$ versus $n$. The associated values of Kolmogorov-Sinai entropy are shown by the solid columns in Fig. 5d.

(ii) Using the relation

$$h = \lim_{n\to\infty} h^{(n)} \tag{34}$$

via the asymptotic behaviour of the Shannon $n$-block entropy per letter depicted in Fig. 5b. The corresponding Kolmogorov-Sinai-entropy values are shown in Fig. 5d by the dotted columns. For both estimates we observe a systematic drop of the entropy of the source in the bursts B1, B2 and B3.

The observed behaviour implies that the average amount of information necessary to predict the next symbol, when being informed about the complete pre-history of the system, significantly decreases in the emerged candidate kHz EM precursor with respect to the noise.

The question arises as to whether the observed asymptotic linear scaling in Figs. 5a is a law of nature. This is an open problem.

*Brief conclusion.* The various block entropies, which quantify dynamic aspects of a time series in a statistical manner, can recognize and discriminate the emerged strong EM precursors from the background noise. They suggest that the memory (or compressibility) in the bursts B1, B2, and B3 is significantly larger in comparison to that of the noise N.

### 4.2 Dynamical characteristics of pre-seismic kHz EM activity in terms of Tsallis entropy

Tsallis entropies are computed using the technique of lumping for binary partition (with the mean value as threshold) and block (word) length $n = 2$. A detailed calculation of Tsallis entropies by means of symbolic dynamics is given in Kalimeri et al. (2008).

As Tsallis (1988) has pointed out, the results depend upon the entropic index $q$ and it is expected that, in every specific case, better discrimination is achieved with appropriate ranges of values of $q$. The appropriate choice of this parameter remains an open problem which we will focus on here.

Recently, Sotolongo-Costa and Posadas (2004) introduced a model for EQ dynamics rooted in a nonextensive framework starting from first principles. They obtained the following analytic expression for the distribution of EQ magnitudes:

$$\log(N(m>)) = \log N + \left(\frac{2-q}{1-q}\right) \times$$

$$\log\left[1+\alpha(q-1)\times(2-q)^{(1-q)/(q-2)}10^{2m}\right] \tag{35}$$

where $N$ is the total number of EQs, $N(m>)$ the number of EQs with magnitude larger than $m$, and $m \approx \log(\varepsilon)$. This is not a trivial result, and incorporates the characteristics of nonextensivity into the magnitude distribution of EQs. The parameter $\alpha$ is the constant of proportionality between the EQ energy and the size of fragment, $r$. Vilar et al. (2007) have revised the fragment-asperity interaction model introduced by Sotolongo-Costa and Posadas by considering a different definition for mean values in the context of Tsallis nonextensive statistics and introducing a new scale between the EQ energy and the size of fragments.

Sotolongo-Costa and Posadas (2004), Silva et al. (2006) and Vilar et al. (2007) successfully tested the viability of this distribution function with data in various different areas. The associated nonextensive parameter found to be distributed in a narrow range from 1.60 to 1.71.

Notice, we have shown (Papadimitriou et al., 2008) that the above mentioned nonextensive models also describe the sequence of pre-seismic kHz EM fluctuations detected prior to the Athens EQ ($M = 5.9$) of 7 September 1999. The associated parameter $q$ is 1.80. In Part 2 of this contribution (Eftaxias et al., 2009b) we will show that the recorded kHz EM fluctuations prior to the L'Aquila EQ can also be described by the revised nonextensive fragment-asperity interaction model (Silva et al., 2006, with a $q$-value of 1.82.

It is very interesting to observe the similarity in the $q$-values for all the groupings of EQs used, as well as for the precursory sequences of kHz EM bursts associated with the activation of the Athens and L'Aquila faults. *This finding is in full agreement with the well documented self-affine nature of faulting and fracture*.

Based on the concepts discussed above, we estimate the Tsallis entropies, with a $q$-value of 1.8. Figure 6 shows that the Tsallis entropies in the emerged strong EM bursts drop to lower values in comparison to that of the noise. This suggests that in the noise there are many kinds of patterns, while in the bursts there are fewer patterns.

Figure 7b compares the Tsallis and Shannon entropies for the excerpts under study. Both entropies give comparable results and clearly discriminate the anomalies from the noise. However, the Shannon entropy makes no connection with the possible physical mechanism involved. The Tsallis entropies at least allow for the possible effects of long-range interaction, long-time memories or multi-fractals.

### 4.3 Dynamical characteristics of pre-seismic kHz EM activity in terms of $T$-entropy

Figure 8 shows that the average $T$-entropies in the emerged kHz EM activity dramatically drop to lower values.

This experimental finding indicates that a significantly lower number of production steps are required in order to construct the string from its alphabet into the emerged strong EM bursts: the bursts are characterized by a considerably lower complexity in comparison to that of the normal epoch (EM background).

*Brief conclusion.* All the tools we have used here, rooted in the notion of symbolic dynamics, discriminate and distinguish in a sensitive way the kHz EM anomalies from the EM background. All the methods we have applied lead to the conclusion that the kHz EM bursts that emerged a few tens of hours prior to the L'Aquila EQ are characterized by a significantly lower complexity (or higher organization, higher predictability, lower uncertainty, and higher compressibility) with respect to that of the EM background (noise).

We consider whether other tools, referring only to the raw data and not to corresponding symbolic sequences, also lead to this conclusion. An answer is given in the following section, where we analyze the data by means of approximate entropy.

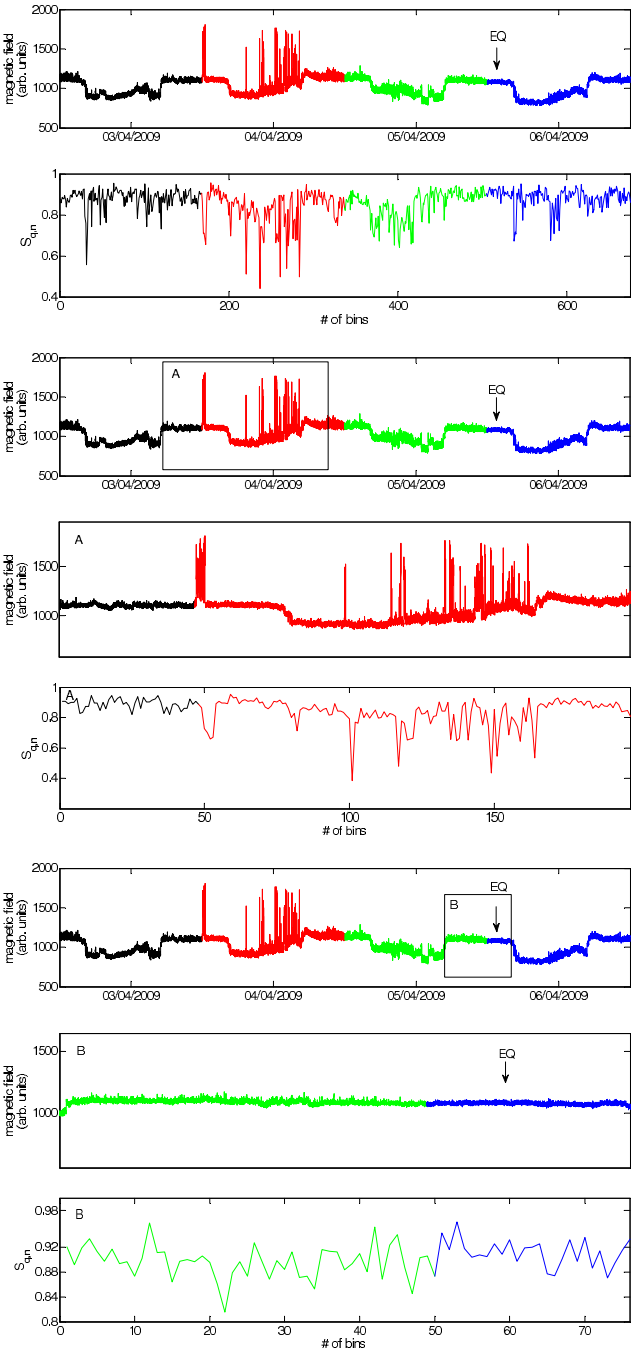


**Fig. 6.** The normalized Tsallis entropy has significantly lower values in the candidate EM precursors B1, B2, and B3 in comparison to that of the noise N. We conclude that the bursts B1, B2, and B3 are characterized by higher organization compared to the noise N.

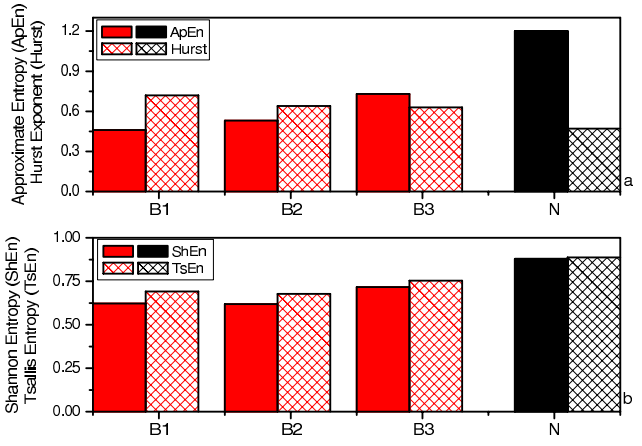


**Fig. 7.** For reasons of comparison, we present the values of $ApEn$, the Hurst exponent estimated by R/S analysis, and Tsallis entropy and Shannon entropy for B1, B2, B3 and N.

### 4.4 Dynamical characteristics of pre-seismic kHz EM activity in terms of approximate entropy

Figure 7a shows that the approximate entropy in the three emerged kHz EM bursts prior to the L'Aquila EQ clearly drops to lower values in comparison to that of the noise.

*The above mentioned result suggests that the candidate kHz EM precursors are governed by the presence of repetitive patterns, which render them more predictable than noise in which such repetitive patterns are absent. Thus, the application of approximate entropy verifies the conclusions extracted by the tools of symbolic dynamics.*

In order to extract more and perhaps different information that may be hidden in the recorded kHz EM anomaly, we shall study the data in terms of fractal spectral analysis in the next section.

### 4.5 Dynamical characteristics of pre-seismic kHz EM activity in terms of fractal spectral analysis

The power spectral densities were estimated using a moving window of 256 samples and an overlap of 255 samples. The spectral parameters $r$ and $\beta$ were calculated for each window.

Figure 9 shows that in the strong kHz EM bursts which emerged on 4 April 2009, the coefficient $r$ takes values very close to 1, i.e., the fit to the power-law is excellent. This is a strong indicator of the fractal character of the underlying processes and structures.

The $\beta$ exponent takes on high values, i.e. between 2 and 3, in the strong EM fluctuations. This fact implies the following:

(i) The EM bursts have long-range temporal correlations, i.e. strong memory: the current value of the precursory signal is correlated not only with its most recent values but also with its long-term history in a scale-invariant, fractal manner. In short, the data indicate an underling mechanism of high organization. Such a mechanism is compatible with the last stage of EQ generation.

(ii) The spectrum manifests more power at lower frequencies than at high frequencies. The enhancement of lower frequency power physically reveals a predominance of larger fracture events. This footprint is also in harmony with the final step of EQ preparation.

(iii) Two classes of signal have been widely used to model stochastic fractal time series, fractional Gaussian (fGn) and fractional Brownian motion (fBm) (Heneghan and McDarby, 2000). For the case of the fGn-model the scaling exponent $\beta$ lies between $-1$ and 1, while the fBm regime is indicated by $\beta$ values from 1 to 3 (Heneghan and McDarby, 2000). The $\beta$ exponent successfully distinguishes the candidate precursory

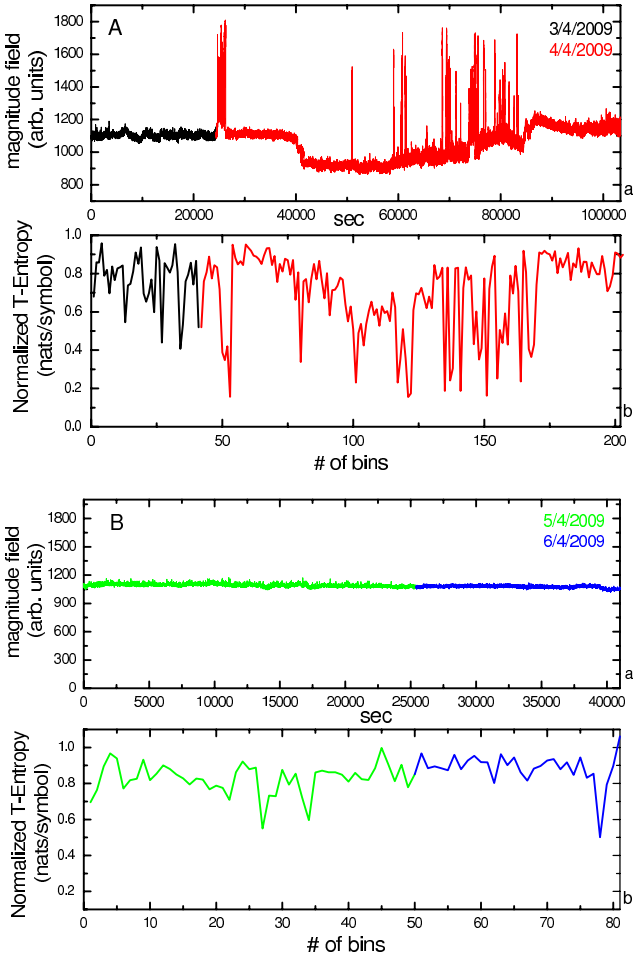


**Fig. 8.** Values of normalized $T$-entropy for time intervals A and B (upper and lower panels, respectively). Time intervals A and B are defined in Fig. 6. In the case of bursts we observe that less production steps are required in order to construct the string from its alphabet.

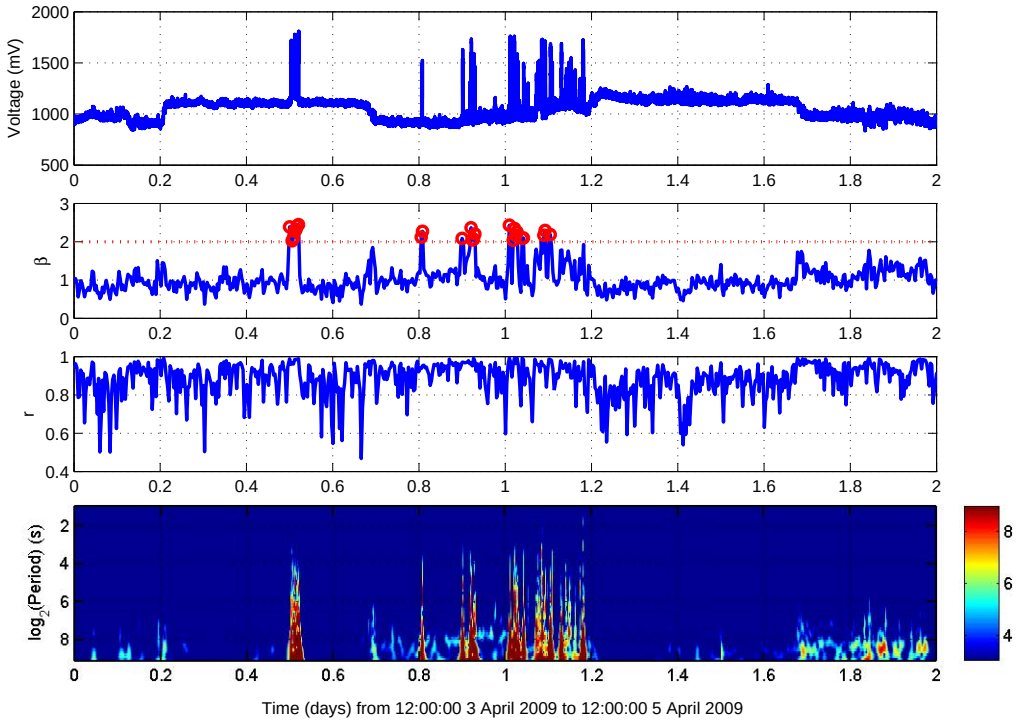


**Fig. 9.** From top to bottom are shown the 10 kHz time series, spectral exponents $\beta$, linear correlation coefficients $r$, and the wavelet power spectrum from 12:00:00 3 April 2009 to 12:00:00 5 April 2009, correspondingly. The red dashed line in the $\beta$ plot marks the transition between anti-persistent and persistent behavior.

activities from the EM noise. Indeed, the $\beta$ values in the EM background are between 1 and 2 indicating that the time profile of the EM time series during the quiet periods is qualitatively analogous to the fGn class. On the contrary, the $\beta$ values in the candidate EM precursors are between 2 and 3, suggesting that the profile of the time series associated with the candidate precursors is qualitatively analogous to the fBm class.

Let's look at the implications of these results.

(i) Theoretical and laboratory experiments support the consideration that both temporal and spatial activity can be described as different cuts in the same underlying fractal (Maslov et al., 1994; Ponomarev et al., 1997). A time series of a major historical event could have both temporal and spatial correlations.

(ii) It has been pointed out that fracture surfaces can be represented by self-affine fractional Brownian surfaces over a wide range (Huang and Turcotte, 1988).

Statements (i) and (ii) lead to the hypothesis that the fBm-type profile of the precursory EM time series reflects the slipping of two rough, rigid Brownian profiles one over the other that led to the L'Aquila EQ nucleation. In Part 2 of this paper this consideration is investigated in detail (Eftaxias et al., 2009b).

The $\beta$ exponent is related to the Hurst exponent $H$ (Hurst, 1951) by the formula (*Turcotte*, 1997):

$$\beta = 2H + 1 \tag{36}$$

with $0 < H < 1$ ($1 < \beta < 3$) for the fractional Brownian motion (fBm) model (Heneghan and McDarby, 2000). The exponent $H$ characterizes the persistent/anti-persistent properties of the signal.

The range $0.5 < H < 1$ ($2 < \beta < 3$) indicates persistency, which means that if the amplitude of the fluctuations increases in a time interval it is likely to continue increasing in the next interval. We recall that we found $\beta$ values in the candidate EM precursors to lie between 2 and 3. The $H$ values are close to 0.7 in the strong segments of the kHz EM activity. This means that their EM fluctuations are positively correlated or persistent, which suggests that the underlying dynamics is governed by a positive feedback mechanism. External influences would then tend to lead the system out of equilibrium (Telesca and Lasaponara, 2006). The system acquires a self-regulating character and, to a great extent, the property of irreversibility, one of the important components of prediction reliability (Morgounov, 2001). Sammis and Sornette (2002) have recently presented the most important positive feedback mechanisms.

*Remark*: the $H$ exponent also reveals the "roughness" of the time series. We draw attention to the fact that the

$H$ values in the strong kHz EM fluctuations are close to the value 0.7. Fracture surfaces were found to be self-affine over a wide range of length scales (Mandelbrot, 1982). The Hurst exponent $H\sim0.75$ has been interpreted as a universal indicator of surface roughness, weakly dependent on the nature of the material and on the failure mode (Lopez and Schmittbuhl, 1998; Hansen and Schmittbuhl, 2003; Ponson et al., 2006). *So, the roughness of the temporal profile of strong pre-seismic kHz anomalies that emerged prior to the L'Aquila EQ reflects the universal spatial roughness of fracture surfaces.* In Part 2 we especially focus on this crucial point.

Hurst (1951) proposed the R/S method in order to identify, through the $H$ exponent, whether the dynamics is persistent, anti-persistent or uncorrelated. We consider whether the R/S method verifies the values of the $H$ exponent estimated by fractal spectral analysis.

### 4.6 Dynamical characteristics of pre-seismic kHz EM activity in terms of R/S analysis

Figure 7a shows that the R/S technique applied directly to the raw data may be of use in distinguishing "candidate pathological" from "healthy" data sets in terms of the $H$ exponent. The "healthy" data (EM background) are characterized by antipersistency. In contrast, the "candidate pathological" data sets are characterized by strong persistency.

We emphasize, that the $H$ exponents derived from the relation $\beta$=2$H$+1, follow quite nicely those estimated by the R/S analysis. Notice, the relation $\beta$=2$H$+1 is valid for the fBm-model. The observed consistency supports the hypothesis that the candidate EM precursors follow the persistent fBm-model. In the next section we examine whether the DFA analysis verifies or not the former hypothesis.

### 4.7 Dynamical characteristics of pre-seismic kHz EM activity in terms of DFA analysis

We fit the experimental time series by the function $F(n)\sim n^{\alpha}$. In a $\log F(n)-\log n$ representation this function is a line with slope $\alpha$. We note that the scaling exponent $\alpha$ is not always constant (independent of scale) and *crossovers* often exist, i.e., the value of $\alpha$ differs for long and short time scales. In order to examine the probable existence of *crossover* behaviour, both the short-term and long-term scaling exponents $\alpha_1$ and $\alpha_2$ were included in the fits for the noise N and the bursts B1, B2, and B3.

Following Peng et al. (1995), we show in Fig. 10 the scatter plot of scaling exponents $\alpha_1$ and $\alpha_2$. The behaviour of these two exponents clearly separates the EM noise from candidate EM precursors. The three bursts are characterized by much larger $\alpha_1$ and $\alpha_2$ values. More precisely, in the noise the two exponents have values close to 1 indicating an underlying $1/f$-type noise, whereas the three bursts have both exponents fairly close (1.5) to that of a fBm-model (Peng et al., 1995).

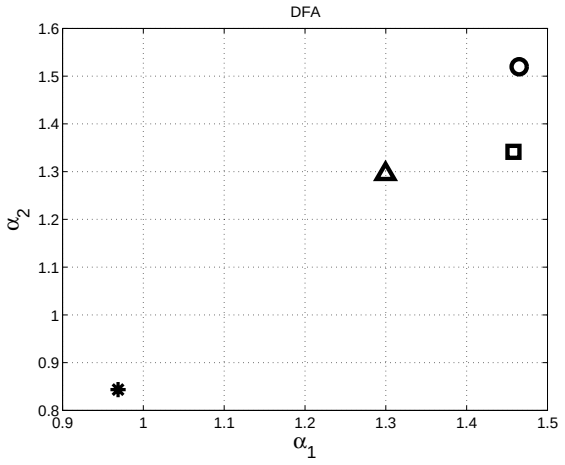


**Fig. 10.** The scatter plot of scaling exponents $\alpha_1$ and $\alpha_2$ clearly separates the EM noise N (denoted by a star) from candidate EM precursors B1 (square), B2 (triangle), and B3 (circle). In the noise the two exponents have values close to 1, indicative of an underlying $1/f$-type noise. In contrast, the three bursts show exponents between 1.3 and 1.5, fairly close to that of fBm ($\alpha_2\sim1.5$).

This finding: (i) supports the conclusion that kHz EM impulsive fluctuations are governed by strong long-range power-law correlations; (ii) indicates an underlying positive feedback mechanism, which, under external influences, has the propensity to lead the system out of equilibrium; (iii) verifies that the strong kHz activity follows the persistent fBm-model.

Notice, the DFA-analysis shows that the candidate EM precursor do not exhibit a clear crossover in scaling behaviour. Indeed, both the $\alpha_1$ and $\alpha_2$ exponents have values pretty close to that (1.5) of a persistent fBm-model.

## 5 View of candidate precursory patterns in terms of complexity theory

The field of study of complex systems holds that the dynamics of complex systems is founded on universal principles that may be used to describe disparate problems ranging from particle physics to the economies of societies (Stanley, 1999, 2000; Stanley et al., 2000; Vicsek, 2001, 2002).

The study of complex system in a unified framework has become recognized in recent years as a new scientific discipline, the ultimate of interdisciplinary fields. For example, de Arcangelis et al. (2006) presented evidence for universality in solar flares and EQ occurrences. Picoli et al. (2007) reported similarities between the dynamics of geomagnetic signals and heartbeat intervals. Kossobokov and Keilis-Borok (2000) have explored similarities of multiple fracturing on a neutron star and on the Earth, including power-law energy distributions, clustering, and the

symptoms of transition to a major rupture. Sornette and Helmstetter (2002) have presented occurrence of finite-time singularities in epidemics, of rupture earthquakes and starquakes. Kapiris et al. (2005) and Eftaxias et al. (2006) reported similarities in precursory features in seismic shocks and epileptic seizures. Osario et al. (2007) have suggested that an epileptic seizure could be considered as a quake of the brain. Fukuda et al. (2003) reported similarities between communication dynamics on the Internet and the automatic nervous system. A common denominator of the various examples of crises is that they emerge from a collective process: the repetitive actions of interactive nonlinear influences on many scales lead to a progressive built-up of large-scale correlations and ultimately to the crisis.

Breaking down the barriers between physics, chemistry, biology and the so-called soft sciences of psychology, sociology, economics, and anthropology, this approach explores the universal physical and mathematical principles that govern the emergence of complex systems from simple components (Bar-Yan, 1997; Sornette, 2002; Rundle et al., 1995).

One of the issues that we will need to address is whether the crucial pathological symptoms of low complexity and persistency included in the candidate kHz EM precursor also characterize other catastrophic events, albeit different in nature.

We investigate the probable presence of such pathological symptoms in epileptic seizures, magnetic storms and solar flares.

### 5.1 Similarities between the dynamics of magnetic storms and EM precursors

Intense magnetic storms are undoubtedly among the most important phenomena in space physics, involving the solar wind, the magnetosphere the ionosphere, the atmosphere and occasionally the Earth's crust (Daglis, 2001; Daglis et al., 2003). The Dst index is a geomagnetic index which monitors the world-wide magnetic storm level. It is based on the average value of the horizontal component of the Earth's magnetic field measured hourly at four near-equatorial geomagnetic observatories.

Recently, Balasis et al. (2006, 2008, 2009a, b) studied Dst data which included intense magnetic storms, as well as a number of smaller events. They have applied the majority of the techniques used in the present work to these events. The results show that all the crucial features extracted from the kHz EM activity in the present paper, including (e.g., long-range correlations, persistency, and the appearance of fluctuations at all scales with a simultaneous predominance of large events), are also contained in intense magnetic storms. We suggested that the development of both intense magnetic storms and kHz EM precursors can study within the unified framework of *Intermittent Criticality*. *Intermittent Criticality has a more general character than classical Self-Organized Criticality, since it implies the predictability of impending catastrophic events.*

In Part 2 of this paper more quantitative evidence of universal behaviour between the kHz EM precursors under study and intense magnetic storms is presented. We emphasize that, based on previously detected kHz EM pre-seismic anomalies, we have already shown that kHz EM precursors and magnetic storms share common scale-invariant natures (Papadimitriou et al., 2008; Balasis et al., 2009a). The relevant analysis is based on the nonextensive model of EQ dynamics presented by Sotolongo-Costa and Posadas (2004).

### 5.2 Similarities between epileptic seizures and EM precursors

Theoretical studies suggest that EQs and neural-seizure dynamics should have many similar features and could be analyzed within similar mathematical frameworks (Hopfield et al., 1994; Rudle et al., 1995; Herz and Hopfield, 1995). Recently, we studied the temporal evolution of the fractal spectral characteristics in: (i) electroencephalograph (EEG) recordings in rat experiments, including epileptic shocks, and (ii) pre-seismic kHz EM time series detected prior to the Athens EQ. We showed that similar distinctive symptoms (including high organization and persistency) appear in epileptic seizures and kHz EM precursors (Kapiris et al., 2005; Eftaxias et al., 2006). We proposed that these two observations also find a unifying explanation within "Intermittent Criticality".

### 5.3 Similarities between solar flares and EM precursors

In a recent work Koulouras et al. (2009) investigated MHz EM radiations rooted in solar flares. A comparative study show that these emissions include all the precursory features extracted from the kHz EM emission under study via fractal spectral analysis. Significantly, the solar activity follows the "persistent fBm model", while persistent behaviour is not found in quiet Sun observations. Schwarz et al. (1998) showed that the time profiles of solar mm-wave bursts are qualitatively analogous to fBm-model, showing persistent behaviour. De Arcangelis et al. (2006) presented evidence for universality in solar flares and EQ occurrences, while Papadimitriou et al. (2008) reported indications for universality in kHz pre-seismic EM activities and EQs.

In a forthcoming paper we report a successful test of the universal hypothesis on solar flares and the kHz EM anomalies detected prior to the L'Aquila EQ. The relevant analysis is based in part on the nonextensive model of EQ dynamics presented by (Solotongo-Costa and Posadas, 2004).

*In summary, the kHz EM precursors under study, epileptic seizures, solar flares, and magnetic storms contain "universal" symptoms in their internal structural patterns. These symptoms clearly distinguish these catastrophic events from the corresponding normal state.*

## 6 Discussion and conclusions

A sequence of ULF, kHz and MHz EM anomalies were recorded at Zante station, from 26 March 2009 up to 4 April 2009, prior to the L'Aquila EQ that occurred on 6 April 2009. "Are there credible earthquake precursors?" is a question debated in the science community. This paper focuses on the question of whether the recorded anomalies are seismogenic or not. Our approach is based on the following key open questions: (i) *How can we recognize an EM observation as a pre-seismic one?* (ii) *How can we link an individual EM precursor with a distinctive stage of the EQ preparation process?* (iii) *How can we identify precursory symptoms in EM observations that indicate that the occurrence of the EQ is unavoidable?* We study the possible seismogenic origin of the anomalies recorded prior to the L'Aquila EQ within the frame work of these open questions. The entire procedure unfolds in two consecutive parts. Here, in Part 1 of our contribution, we restrict ourselves to the study of the kHz EM anomalies, which have a crucial role in addressing the above three challenges. More precisely, we focus on the question whether the recorded kHz EM anomalies are seismogenic or not.

In order to develop a quantitative identification of a kHz EM anomaly, measures of entropy and tools of information theory have been used to identify statistical patterns; a significant change of these patterns represents a deviation from normal behaviour, revealing the presence of an anomaly. *In principle one cannot find an optimum tool for anomaly detection*. A combination of various tools seems to be the best way to get a more precise characterization of a recorded anomaly as pre-seismic.

We analyzed the kHz EM time series in terms of Shannon $n$-block entropy, Shannon $n$-block entropy per letter, conditional entropy, entropy of the source, nonextensive Tsallis entropy and $T$-entropy, which refer to a transformed symbolic sequence. For the purpose of comparison we applied one more tool, approximate entropy which refers directly to the raw data. We conclude that all the methods applied are sensitive in distinguishing the launched candidate kHz radiation from the normal background state (noise). *the kHz EM anomalies are characterized by a considerably lower complexity (higher organization, lower uncertainty, higher predictability and higher compressibility) in comparison to that of the background.*

The spectral fractal technique further distinguishes the candidate kHz EM precursor from the background. *The former follows the persistent fractional Brownian motion model, while the noise the fractional Gaussian noise model*. We verify the existence of persistency in the anomalies by R/S analysis. The indication that the candidate precursor follows the fractional Brownian motion model is verified by means of detrended fractal analysis.

The fact that the launch of anomalies from the normal state is combined by a simultaneous appearance of: (i) a significantly higher level of organization, and (ii) persistency, indicates that the process, in which the anomalies are rooted, is governed by a *positive feedback mechanism*. Such a mechanism is consistent with the anomalies being a candidate precursor. The existence of a positive feedback mechanism expresses a positive circular causality that acts as a growth-generating phenomenon and therefore drives unstable patterns (Telesca and Lasaponara, 2006). It can be the result of stress transfer from damaged to intact entities or it can result from the effect of damage in lowering the local elastic stiffness (Sammis and Sornette, 2002). The appearance of the property of irreversibility in a probable precursor is one of the important components of predictive capability (Morgounov, 2001).

In this field of research, the reproducibility of results is desirable. Significantly, the catastrophic symptoms found in the candidate kHz EM precursors under study are also found in rather well established kHz EM precursors associated with significant EQ that recently occurred in Greece (e.g. Kapiris et al., 2004; Contoyiannis et al., 2005; Eftaxias et al., 2007; 2008; Kalimeri et al., 2008).

The study of complex systems holds that the dynamics found in such systems is rooted in universal principles that may be used to describe disparate problems ranging from particle physics to the economies of societies. Evidence has shown that high organization and persistency footprints are also included in other catastrophic events, such as neural-seizures, magnetic storms, and solar flares. Part 2 of this communication further supports the hypothesis that such phenomena can be investigated in a unified framework (Eftaxias et al., 2009b).

We consider whether the clear discrimination of the kHz EM anomalies that emerged from the normal state prior to the L'Aquila EQ, even based on a combination of (i) a rather strong statistical analysis and (ii) striking similarities with other complex catastrophic events, leads reliably to the conclusion that these anomalies were rooted in the preparation of the L'Aquila EQ.

Our view is that such an analysis by itself cannot establish an anomaly as a precursor. It likely offers *necessary* but not *sufficient* criteria in order to recognize an EM anomaly as pre-seismic.

Much remains to be done to tackle precursors systematically. It is a difficult task to rebate two events separated in time, such as a candidate EM precursor and the ensuing EQ. It remains to be established whether different approaches could provide additional information that would allow one to accept the seismogenic origin of the recorded kHz EM anomalies and link these to a corresponding stage of EQ generation.

In Part 2 (Eftaxias et al., 2009b), based on the strategy described in the Introduction, we complete our study. We support the seismogenic origin of the detected kHz-MHz EM anomalies. In particular, we focus on the questions: *How can we link an individual EM precursor with a distinctive*

*stage of the EQ preparation process? How can we identify precursory symptoms in EM observations that indicate that the occurrence of the EQ is unavoidable?* We will argue that:

(i) The kHz EM anomalies were associated with the fracture of asperities that were distributed along the L'Aquila fault sustaining the system. The aspect of self-affine nature of faulting and fracture is widely documented from both, field observations and laboratory experiments, and studies of failure precursors on the small (laboratory) and large (earthquake) scale. It is expected that this fundamental aspect bridges the regional seismicity with activation of a single fault, on one hand, and the activation of a single fault with laboratory seismicity, on the other hand. We verify this prospect in terms of the detected kHz EM precursor. We show that the activation the L'Aquila is a reduced self-affine image of the regional seismicity and a magnified image of laboratory seismicity. Furthermore, ample experimental and theoretical evidence especially support the hypothesis that natural rock surfaces can be represented by a fractional Brownian motion scheme over a wide range. We show that the universal fractional Brownian motion spatial profile of the L'Aquila fault has been mirrored into the candidate precursory kHz EM activity. We paid attention to the fact that the surface roughness has been interpreted as a universal indicator of surface fracture, weakly dependent on the nature of the material and on the failure mode. We conclude that the universal spatial roughness of fracture surfaces pretty coincides with the roughness of the temporal profile of the kHz EM anomaly that emerged a few tens of hours prior to the L'Aquila EQ.

(ii) The MHz EM anomalies could be triggered by fractures in the highly disordered system that surrounded the backbone of asperities of the activated fault. Fracture process in heterogeneous materials is characterized by antipersistency, and can be described in analogy with a thermal continuous second order phase transition. We show that these two crucial features are mirrored on the MHz EM candidate precursor.

(iii) We clearly state that the detection of a MHz EM precursor does not mean that the occurrence of EQ is unavoidable The abrupt emergence of kHz EM emissions indicate the fracture of asperities.

*Acknowledgements.* We thank Mioara Mandea and two anonymous reviewers for their constructive comments and remarks.

Edited by: P. F. Biagi
Reviewed by: M. Mandea and two other anonymous referees

## References

Andersen, J., Sornette, D., and Leung, K.: Tricritical behaviour in iupture Induced by disorder, Phys. Rev. Lett., 78, 2140–2143, 1997.

de Arcangelis, L., Godano, C., Lippiello, E., and Nicodemi, M.: Universality in Solar Flare and Earthquake Occurrence, Phys. Rev. Lett., 96, 051102/1–4, 2006.

Bahat, D., Rabinovitch, A., and Frid, V.: Tensile fracturing in rocks: Tectonofractographic and Electromagnetic Radiation Methods, Springer Verlag, Berlin, 570 pp., 2005.

Balasis, G., Daglis, I., Kapiris, P., Mandea, M., Vassiliadis, D., and Eftaxias, K.: From pre-storm activity to magnetic storms: a transition described in terms of fractal dynamics, Ann. Geophys., 24, 3557-3567, 2006, http://www.ann-geophys.net/24/3557/2006/.

Balasis, G., Daglis, I., Papadimitriou, C., Kalimeri, M., Anastasiadis, A., and Eftaxias, K.: Dynamical complexity in Dst time series using non-extensive Tsallis entropy, Geophys. Res. Lett., 35, L14102, doi:10.1029/2008GL034743, 2008.

Balasis, G. and Eftaxias, K.: A study of non-extensivity in the Earths magnetosphere, European Physical Journal, 174, 219-225, 2009a.

Balasis, G., Daglis, I., Papadimitriou, C., Kalimeri, M., Anastasiadis, A., and Eftaxias, K.: Investigating dynamical complexity in the magnetosphere using various entropy measures, J. Geophys. Res., 114, A00D06 (13 pp.), doi:10.1029/2008JA014035, 2009b.

Bar-Yan, Y.: Dynamics of complex systems, Addison-Wesley, Reading, Massachusetts, 849 pp., 1997.

Biagi, P., Castellana, L., Maggipinto, T., Loiacono, D., Schiavulli, L., Ligonzo, T., Fiore, M., Suciu, E., and Ermini, A.: A pre seismic radio anomaly revealed in the area where the Abruzzo earthquake ($M$=6.3) occurred on 6 April 2009, Nat. Hazards Earth Syst. Sci., 9, 1551-1556, 2009, http://www.nat-hazards-earth-syst-sci.net/9/1551/2009/.

Bowman, D., Ouillon, G., Sammis, C., Sornette, A., and Sornette, D.: An observational test of the critical earthquake concept, J. Geophys. Res., 103, 24359-24372, 1998.

Contoyiannis, Y. and Diakonos, F.: Criticality and intermittency in the order parameter space, Phys. Lett. A, 268, 286–272, 2000.

Contoyiannis, Y., Diakonos, F., and Malakis, A.: Intermittent dynamics of critical fluctuations, Phys. Rev. Lett., 89, 35701–35704, 2002.

Contoyiannis, Y., Kapiris, P., and Eftaxias, K.: Monitoring of a preseismic phase from its electromagnetic precursors, Physical Review E, 71, 061123/1–14, 2005.

Contoyiannis, Y. F. and Eftaxias, K.: Tsallis and Levy statistics in the preparation of an earthquake, Nonlin. Processes Geophys., 15, 379–388, 2008.

Daglis, I.: The storm-time ring current, Space Sci. Rev., 98, 323–363, 2001.

Daglis, I., Kozyra, J., Kamide, Y., Vassiliadis, D., Sharma, A., Liemohn, M., Gonzalez, W., Tsurutani, B., and Lu, G.: Intense space storms: Critical issues and open disputes, J. Geophys. Res., 108, 1208, doi:10.1029/2002JA009722, 2003.

Ebeling, W. and Nicolis, G.: Word frequency and entropy of symbolic sequences: A dynamical Perspective, Chaos, Solitons & Fractals, 2, 635–650, 1992.

Ebeling, W.: Prediction and entropy of nonlinear dynamical systems and symbolic sequences with LRO, Physica D, 109, 42–52, 1997.

Ebeling, W., Steuer, R., and Titchener, M.: Partition-based entropies of deterministic and stochastic maps, Stochastics and Dynamics, 1, 45–61, 2001.

Ebeling, W.: Entropies and predictability of nonlinear processes and time series, edited by: Sloot, P. M. A., et al., ICCS 2002, LNCS, 1209–1217, 2002

Eftaxias, K., Kapiris, P., Dologlou, E., Kopanas, J., Bogris, N., Antonopoulos, G., Peratzakis, A., and Hadjicontis, V.: EM anomalies before the Kozani earthquake: A study of their behaviour through laboratory experiments, Geophys. Res. Lett., 29, 69/1–69/4, 2002.

Eftaxias, K., Frangos, P., Kapiris, P., Polygiannakis, J., Kopanas, J., Peratzakis, A., Skountzos, P., and Jaggard, D.: Review and a Model of Pre-Seismic electromagnetic emissions in terms of fractal electrodynamics, Fractals, 12, 243–273, 2004.

Eftaxias, K. A., Kapiris, P. G., Balasis, G. T., Peratzakis, A., Karamanos, K., Kopanas, J., Antonopoulos, G., and Nomicos, K. D.: Unified approach to catastrophic events: from the normal state to geological or biological shock in terms of spectral fractal and nonlinear analysis, Nat. Hazards Earth Syst. Sci., 6, 205–228, 2006, http://www.nat-hazards-earth-syst-sci.net/6/205/2006/.

Eftaxias, K., Sgrigna, V., and Chelidze, T.: Mechanical and Electromagnetic Phenomena Accompanying Preseismic Deformation: from Laboratory to Geophysical Scale, Tectonophysics, 431, 1-301, 2007a.

Eftaxias, K., Panin, V., and Deryugin Y.: Evolution EM-signals before earthquake and during laboratory test of rocks, Tectonophysics, 431, 273-300, 2007b.

Eftaxias, K.: Footprints of nonextensive Tsallis statistics, selfaffinity and universality in the preparation of the L'Aquila earthquake hidden in a pre-seismic EM emission, Physica A, 389, 133–140, 2009a.

Eftaxias, K., Balasis, G., Papadimitriou, C., Contoyiannis, Y., Athanasopoulou, L., Kalimeri, M., Nikolopoulos., S., Kopanas, J., Antonopoulos, G., and Nomicos, C.: Unfolding the procedure of characterizing recorded ultra low frequency, kHZ and MHz electromagnetic anomalies prior to the L'Aquila earthquake as pre-seismic ones – Part 2, Nat. Hazards Earth Syst. Sci., submitted, 2009b.

Fukuda, K., Nunes, L., and Stanley, H.: Similarities between communication dynamics in the Internet and the automatic nervous system, Europhys. Lett., 62, 189–195, 2003.

Gershenzon, N. and Bambakidis, G.: Modelling of seismoelectromagnetic phenomena, Russ. J. Earth Sci., 3, 247–275, 2001.

Grassberger, P. and Procaccia, I.: Characterization of strange attractors, 50, 346–349, 1983.

Gluzman, S. and Sornette, D.: Self-consistent theory of rupture by progressive diffuse damage, Phys. Rev. E., 63, 066129(1–11), 2001.

Graben, P. and Kurths, J.: Detecting subthreshold events in noisy data by symbolic dynamics, Phys. Rev. Lett., 90, 100602(1–4), 2003.

Hansen, A. and Schmittbuhl, J.: Origin of the universal roughness exponent of brittle fracture surfaces: stress-weighted percolation in the damage zone, Phys. Rev. Lett., 90, 45504-45507, 2003.

Hao, B.-L.: Elementary symbolic dynamics and chaos in dissipative systems, World Scientific, 476 pp., 1989.

Hao, B.-L.: Symbolic dynamics and characterization of complexity, Physica D, 51, 161–176, 1991.

Hayakawa, M. and Fujinawa, Y.: Electromagnetic Phenomena Related to Earthquake Prediction, Terrapub, Tokyo, 1994.

Hayakawa, M.: Atmospheric and Ionospheric Electromagnetic Phenomena Associated with Earthquakes, Terrapub, Tokyo, 1999.

Hayakawa, M. and Molchanov, O.: Seismo Electromagnetics, Terrapub, Tokyo, 2002.

Henegham, C. and McDarby, G.: Establishing the relation between detrended fluctuation analysis and power spectral density analysis foe stochastic processes, Phys. Rev. E, 62, 6103–6110, 2000.

Herrmann, H. J. and Roux, S.: Statistical Physics for the Fracture of Disordered Media, Elsevier, Amsterdam, 1990.

Herz, A. and Hopfield, J.: Earthquake cycles and neural reverberations: Collective oscillations in systems with pulse-coupled threshold elements, Phys. Rev. Lett., 75, 1222-1225, 1995.

Hopfield, J.: Neurons, dynamics and computation, Phys. Today, 40, 40-46, 1994.

Huang, J. and Turcotte, D.: Fractal distributions of stress and strength and variations of b value, Earth Planet. Sc. Lett., 91, 223-230, 1988.

Hurst, H.: Long term storage capacity of reservoirs, Trans. Am. Soc. Civ. Eng., 116, 770-808, 1951.

Johansen, A. and Sornette, D.: Critical ruptures, European Physics Journal B, 18, 163–181, 2000.

Kalimeri, M., Papadimitriou, C., and Eftaxias, K.: Dynamical complexity detection in pre-seismic emissions using nonadditive Tsallis entropy, Physica A, 387, 1161–1172, 2008.

Kapiris, P., Eftaxias, K., and Chelidze, T.: The electromagnetic signature of prefracture criticality in heterogeneous media, Phys. Rev. Lett., 92, 065702/1-4, 2004.

Kapiris, P., Polygiannakis, J., Li, X., Yao, X., and Eftaxias, K.: Similarities in precursory features in seismic shocks and epileptic seizures, Europhys. Lett., 69, 657–663, 2005.

Karamanos, K. and Nicolis, G.: Symbolic Dynamics and Entropy Analysis of Feigenbaum Limit Sets, Chaos, Solitons & Fractals, 10(7), 1135–1150, 1999.

Karamanos, K.: From symbolic dynamics to a digital approach: Chaos and Transcendence, Lect. Notes in Phys., 550, 357–371, 2000.

Karamanos, K.: Entropy analysis of substitutive sequences revisited, J. Phys. A: Math. Gen., 34, 9231–9241, 2001.

Karamanos, K., Dakopoulos, D., Aloupis, K., Peratzakis, A., Athanasopoulou, L., Nikolopoulos, S., Kapiris, P., and Eftaxias, K.: Study of pre-seismic electromagnetic signals in terms of complexity, Physical Review E, 74, 016104-1/21, 2006.

Khinchin, A. I.: Mathematical Foundations of Information Theory, Dover, New York, 1957.

Kitchens, B.: Symbolic Dynamics, One-Sided, Two-Sided and Countable State Markov Shifts, Springer, 252 pp., 1998.

Koulouras,G., Balasis, G., Kiourktsidis, I., Nannos, E., Kontakos, K., Stonham, J., Ruzhin, Y., Eftaxias, K., Kavouras, D., Nomikos, K.: Discrimination between preseismic electromagnetic anomalies and solar activity effects, Phys. Scripta, 79, 45901(12 pp.), 2009.

Kurths, J., Voss, A., Saparin, P., Witt, A., Kleiner, H., and Wessel., N.: Quantitative analysis of heart rate variability, Chaos, 5,

88–94, 1995.
Lopez, J. and Schmittbuhl, J.: Anomalous scaling of fracture surfaces, Phys. Rev. E, 57, 6405-6408, 1998.
Latora, V. and Baranger, M., Kolmogorov-Sinai Entropy Rate versus Physical Entropy, Phys. Rev. Lett., 82, 520–523, 1999.
Maslov, S., Paczuski, M., and Bak, P.: Avalanches and 1/f Noise in Evolution and Growth Models, Phys. Rev. Lett., 73, 2162–2165, 1994.
Morgounov, V.: Relaxation creep model of impending earthquake, Ann. Geofis., 44(2), 369–381, 2001.
Muto, J., Nagahama, H., Miura, T., and Arakawa, I.: Frictional discharge at fault asperities: origin of fractal seismoelectromagnetic radiation, Tectonophysics, 431, 113–122, 2007.
Osorio, I., Frei, M., Sornette, D., Milton, J., and Lai, Y.: Epileptic Seizures: Quakes of the brain?, arXiv:0712.3929v1, 2007.
Papadimitriou, C., Kalimeri, M., and Eftaxias, K.: Nonextensivity and universality in the earthquake preparation process, Phys. Rev. E., 77, 036101/114, 2008.
Peng, C., Mietus, J., Hausdorff, J., Havlin, S., Stanley, H., and Goldberger, A.: Long-range anticorrelations and non-Gaussian behavior of the heartbeat, Phys. Rev. Lett., 70, 1343–1346, 1993.
Peng, C., Havlin, S., Stanley, H., and Goldberger, A.: Quantification of scaling exponents and crossover phenomena in nonstationary heartbeat timeseries, Chaos, 5, 82-87, 1995.
Picoli, S., Mendes, R., Malacarne, L., and Papa, A.: Similarities between the dynamics of geomagnetic signal and heartbeat intervals, Europhys. Lett., 80, 50006/16, 2007.
Pincus, S.: Approximate Entropy: A Complexity Measure for Biologic Time series Data, Proceedings of IEEE 17th Annual Northeast Bioengineering Conference, IEE Press, New York, 35-36, 1991.
Pincus, S. and Keefe, D.: Quantification of hormone pulsatility via an approximate entropy algorithm, Am. J. Physiol. (Endocrinol Metab) 262, E741-E754, 1992.
Pincus, S. and Goldberger, A.: Physiological time-series analysis: what does regularity quantify?, Am. J. Physiol., 266, H1643–H1656, 1994.
Pincus, S. and Singer, B.: Randomness and degree of irregularity, P. Natl. Acad. Sci. USA, 93, 2083–2088, 1996.
Ponomarev, A., Zavyalov, A., Smirnov, V., and Lockner, D.: Physical modelling of the formation and evolution of seismically active fault zones, Tectonophysics, 277, 57-,81, 1997.
Ponson, L., Bonamy, D., and Bouchaud, E.: Two-dimensional scaling properties of experimental fracture surfaces, Phys. Rev. Lett., 96(3), 035506, doi:10.1103/PhysRevLett.96.035506, 2006.
Rozhnoi, A., Solovieva, M., Molchanov, O., Schwingenschuh, K., Boudjada, M., Biagi, P., Maggipinto, T., and Castellana, L: VLF signal precursor of L'Aquila earthquake, JRA3/EMDAF kick-off meeting, 2009.
Rundle, J., Tiampo, K., Klein, W., and Martins, J. S.: Selforganization in leaky threshold systems: the influence of nearmean field dynamics and its implications for EQ, neurology, and forecasting, P. Natl. Acad. Sci. USA, 99, 2514-2521, 2002.
Sammis, C. and Sornette, D.: Positive feedback, memory, and the predictability of EQ, P. Natl. Acad. Sci. USA, 99, 2501–2508, 2002.
Schwarz, U., Kurths, J., Klien, B., Kruger, A., and Upro, S.: Multiresolution analysis of solar mm-wave bursts, Astron. Astrophys. Suppl. Ser., 127, 309–318, 1998
Shannon, C. E.: A mathematical theory of communication, The Bell System Tech. J., 27, 379–423, 623-656, 1948.
Silva, R., Franca, G., Vilar, C., and Alcaniz, J.: Nonextensive models for earthquakes, Phys. Rev. E, 73, 026102-1/5, 2006.
Sornette, D. and Andersen, J. V.: Scaling with respect to disorder in time-to-failure, Eur. Phys. J. B, 1, 353–357, 1998.
Sornette, D.: Critical Phenomena in Natural Sciences, Chaos, Fractals, Self-organization and Disorder: Concepts and Tools, 2nd edn., Springer Series in Synergetics, Heidelberg, 2004.
Sornette, D.: Predictability of catastrophic events: Material ruptures, EQ, turbulence, financial crashes, and human birth, P. Natl. Acad. Sci. USA, 99, 2522-2529, 2002.
Sornette, D. and Helmstetter, A.: Occurrence of finite-time singularities in epidemic models of rupture, EQ, and starquakes, Phys. Rev. Lett., 89, 158501/1–4, 2002.
Sotolongo-Costa, O. and Posadas, A.: Fragment-asperity interaction model for EQ, Phys. Rev. Lett., 92, 048501/1-4, 2004.
Stanley, H.: Scaling, universality, and renormalization: Three pillars of modern critical phenomena, Rev. Mod. Phys., 71, S358-S366, 1999.
Stanley, H., Amaral, L., Goldberger, A., Havlin, S., Ivanov, P., and Peng, C.: Statistical physics and physiology: Monofractal and multifractal approaches, Physica A, 106, 309-324, 1999.
Stanley, H.: Exotic statistical physics: Applications to biology, medicine, and economics, Physica A, 285, 1-17, 2000.
Steuer, R., Molgedey, L., Ebeling, W., and Jimenez-Montano, M.: Entropy and optimal partition gor data analysis, Eur. Phys. J. B, 19, 265–269, 2001.
Telesca, L. and Lasaponara, R.: Vegetational patterns in burned and unburned areas investigated by using the detredted fluctuation analysis, Physica A, 368, 531–535, 20006.
Titchener, M., Nicolescu, R., Staiger, L., Gulliver, A., and Speidel, U.: Deterministic Complexity and Entropy, Fund. Inform., 64, 443–461, 2005.
Torrence, C. and Compo, G. P.: A Practical Guide toWavelet Analysis, B. Am. Meteorol. Soc., 79, 61-78, 1998.
Tsallis, C.: Possible generalization of Boltzmann-Gibbs statistics, J. Stat. Phys., 52, 479–487, 1988.
Tsallis, C.: Introduction to Nonextensive Statistical Mechanics, Approaching a Complex Word, Springer, 2009.
Turcotte, D.: Fractals and chaos in geology and geophysics, 2nd edn., Cambridge University Press, 398 pp., 1997.
Uyeda, S: In defense of VAN's earthquake predictions, EOS T. Am. Geophys. Un., 81, 3–6, 2000.
Vicsek, T.: A question of scale, Nature, 411, 421 pp., 2001.
Vicsek, T.: The bigger picture, Nature, 418, 131 pp., 2002.
Vilar, C., Franca, G., Silva, R., and Alcaniz, J.: Nonextensivity in geological faults?, Physica A, 377, 285–290, 2007.
Voss, A., Kurths, J., Kleiner, H., Witt, A., Wessel, N., Saparin, N., Osterziel, K., Schurath, R., and Dietz, R.: The application of methods of non-linear dynamics for the improved and predictive recognition of patients threatened by sudden cardiac death, Cardiovascular Research, 31(3), 419–433, 1996.
Zunino, L., Perez, D., Kowalski, A., Martin, M., Garavaglia, M., Plastino, A., and Rosso, O.: Fractional Brownian motion, fractional Gaussian noise and Tsallis permutation entropy, Physica A, 387, 6057–6068, 2008.